IL NUOVO CIMENTO **49 C** (2026) 30
DOI 10.1393/ncc/i2026-26030-7

Colloquia: IFAE 2025

Search for dark photons from Higgs boson decays with the ATLAS detector in the Run 3(*)

Giulia Maineri
Università degli Studi e INFN Milano - Milano, Italy

received 10 October 2025

Summary. — The dark photon is predicted to be the gauge boson of an additional U(1) group of a hypothetical dark sector in some BSM theories. This analysis searches for the dark photon, in the research channel where the Higgs boson decays into a photon and a dark photon, that manifests in the detector as missing transverse momentum. Data collected during the Run 3 of the LHC by the ATLAS detector are used. The analysis focuses on the gluon fusion channel, still unexplored; for this purpose, a dedicated trigger algorithm has been developed, based on 3 variables: transverse momentum of the photon, transverse mass and missing transverse momentum. The Signal Region (SR) is optimised so to improve the sensitivity of the analysis and to reduce the contribution of experimental background, to which many different SM processes contribute, such as $W\gamma$ and $Z\gamma$, and processes where an electron or a jet is mis-reconstructed as a photon. Data-driven techniques to estimate the background processes have been developed specifically for this analysis, using background-enriched Control Regions (CRs). Finally, a simultaneous fit in SR and CRs is performed to extract an upper limit on the Branching Ratio of the $H \to \gamma\gamma_d$ decay.

1. – The Dark Matter problem

The Dark Matter (DM) problem is a fundamental topic in astrophysics and particle physics, corroborated by numerous cosmological evidences and gravitational effects [1] [2] that show the incompleteness of the Standard Model (SM). According to Cosmic Microwave Background (CMB) measurements [3], the DM constitutes $\sim 27\%$ of the total Universe matter and energy density.

An appealing scenario [4] predicts DM to be part of a dark sector, made of many different "dark particles" with their own gauge interactions. In this framework, there should also be a "dark" equivalent of the photon, the dark photon γ_d [5,6], the boson of an additional $U(1)_d$ symmetry group.

The dark and visible sectors may weakly interact through a "portal", offering a potential experimental signature that could be revealed at the Large Hadron Collider (LHC).

One of the possible discovery channels for dark photons at the LHC is the Higgs decay into a photon and a dark photon ($H \to \gamma\gamma_d$). The massless dark photon could couple to

(*) IFAE 2025 - "Energy Frontier" session

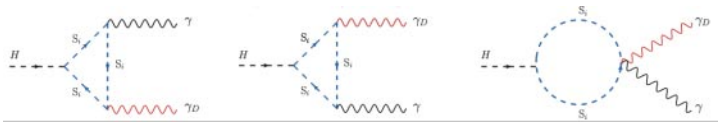

Fig. 1. – Higgs boson decay into a photon and a dark photon could be mediated by a loop of messenger fields S_i.

the Higgs boson through a loop of messenger fields (fig. 1). In a detector such as ATLAS [7], the characteristic signature of such a decay would be a final state with a photon and missing transverse momentum $\vec{p}_T^{miss}$. This quantity takes into account the momentum imbalance in the transverse plane, due to the presence of undetectable particles, such as neutrinos or weakly interacting Beyond Standard Model (BSM) particles.

2. – State of the art

The $H \to \gamma\gamma_d$ analysis is part of a rich program in the ATLAS Collaboration focusing on BSM searches. During Run 2 data taking (2015-2018), the only Higgs production channels that could be studied were the Higgs associated production to a Z boson (ZH) and the Higgs production via Vector Boson Fusion (VBF).

In the ZH channel, the final state is characterized by 1 photon γ, p_T^{miss} due to the undetectable γ_d, and 2 same-flavour opposite-sign leptons ($l \in \{e, \mu\}$), from the decay of the Z boson. Events were selected with single-lepton and dilepton triggers [8,9]. Results of this analysis have been published in 2023 [10]; as no excess with respect to the SM prediction has been observed, an upper limit on the branching ratio BR($H \to \gamma\gamma_d$) has been set at 2.28% at 95% CL.

In the VBF channel, the final state is characterized by two forward hadronic jets and p_T^{miss}. Events were selected with the p_T^{miss} trigger [11] and an offline selection requiring $p_T^{miss} > 150\,\text{GeV}$.

The results of the ZH and VBF analyses have been then combined, in order to get the best observed (expected) exclusion limit on the BR($H \to \gamma\gamma_d$) [12], set at 1.3% (1.5%) for the SM Higgs boson. The combination is allowed by the orthogonality of the two analysis selections, since VBF search vetoes leptons, while ZH search requires 2 leptons.

3. – Run 3 analysis

The Run 3 analysis targets the gluon fusion channel $gg \to H$ (fig. 2), the one with the highest cross-section for Higgs boson production (48.58 pb at 13 TeV, to be compared

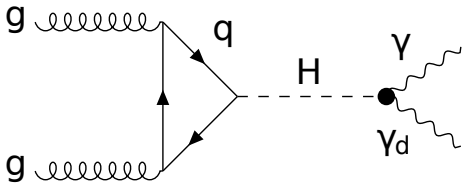

Fig. 2. – Higgs production via gluon fusion diagram.

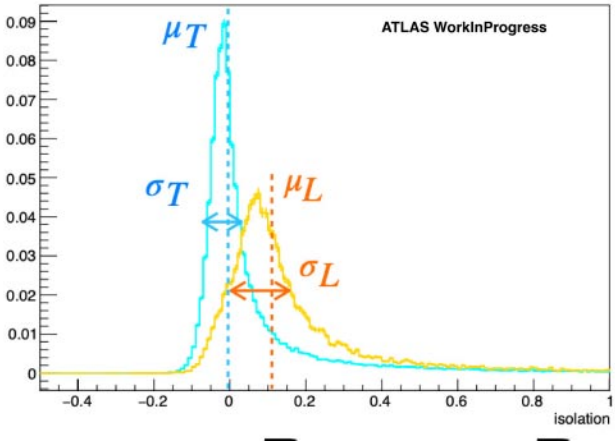

Fig. 3. – Tight and loose γ isolation distributions in Monte Carlo. A L $\rightarrow$T transformation is extracted from MC and then adapted to data.

with the VBF channel, 3.78 pb, and the ZH channel, 0.88 pb [13]). A dedicated composite trigger has been developed to target this channel, requiring three cuts: missing transverse momentum higher than 70 GeV, a tight photon with transverse momentum higher than 50 GeV, and transverse mass m_T between the photon and the missing transverse momentum higher than 80 GeV.

Moreover, a list of cuts on discriminant variables has been optimised in order to increase the sensitivity to the signal, thus defining a Signal Region.

Furthermore, a BDT has been optimised in order to distinguish well-reconstructed and wrongly-reconstructed vertices. Indeed, the presence of a highly energetic photon in the final state, together with missing transverse momentum, results in having low track activity in the final state, thus increasing the probability to pick the wrong primary vertex. A cut on the BDT score allows to recover almost a 100% vertex identification purity for both signal and backgrounds in Signal Region.

4. – Estimation of backgrounds

The Signal Region (SR) is populated by a sizeable background from several Standard Model processes.

$Z(\rightarrow \nu\nu)\gamma$ events, where both the photon and the p_T^{miss} are genuine, represent the irreducible background for the $gg \rightarrow H \rightarrow \gamma\gamma_d$ analysis, while the main reducible backgrounds are γ+jets, multijets, Z+jets, W+jets and $W\gamma$ events. The latter process contributes to the background when the W boson decays to a lepton and a neutrino and the lepton is out of the detector acceptance. Background processes are estimated using different data-driven techniques in proper Control Regions (CRs); Monte Carlo (MC) simulations cannot indeed be fully trusted as the simulation may not be accurate enough in the kinematic regions explored in this search. CRs are constructed inverting one of the cuts defining the SR, *e.g.*, the number of leptons or the photon isolation cut, to guarantee the orthogonality with the SR.

$Z(\rightarrow \nu\nu)\gamma$ and $W\gamma$ MC samples in SR are normalized using k-factors extracted in leptonic CRs, required to contain 2 or 1 muon respectively. In such CRs, muons are

treated as invisible when computing p_T^{miss} and its related variables, so that the kinematics of the 1μ CR is as similar as possible to that of the SR. K-factors accounting for possible mis-modelling of the cross-sections are calculated from the comparison of data and MC simulations in each bin of transverse mass, the discriminant variable that will be used in the likelihood fit.

Multijets, Z+jets and W+jets enter the category of the "jets faking photons" background, *i.e.*, hadronic jets mis-reconstructed as photons. The estimation is done by means of a Non-Isolated CR enriched in jet faking photons, where the photon is required to be not-isolated in the calorimeter. A new data-driven technique that exploit photon isolation as a discriminant between true and fake photons has been developed in order to estimate this background. The photon isolation variable is described by the energy in a cone surrounding the photon divided by the photon energy. Genuine photons are expected to be more isolated than fake photons, that tend to be produced inside hadronic jets, therefore in an environment affected by surrounding hadronic activity. The fake γ isolation distributions have been used to calculate fake factors (eq. 1) as ratios between yields in Isolated and Non-Isolated Regions (fig. 4), later applied to the Non-Isolated CR to obtain the background yield in SR.

$$f = \left(\frac{N_{j \rightsquigarrow \gamma}^{isol}}{N_{j \rightsquigarrow \gamma}^{non-isol}} \right)_{tight} \tag{1}$$

In order to compute the ratio in eq.1, the isolation distribution of fake tight photons in data is needed. Isolation is indeed typically not well modelled by MC simulations for jets faking photons. As this isolation distribution is unknown (in data it is not possible to distinguish true and fake photons), a new extrapolation method has been developed in order to extract it. The key idea of the extrapolation method is that the tight fake photons isolation distribution can be obtained from the isolation distribution of another sample of photons not passing the "tight" identification - called "loose" photons. Some assumptions are made: loose photons in data are mostly fake; the transformation (L

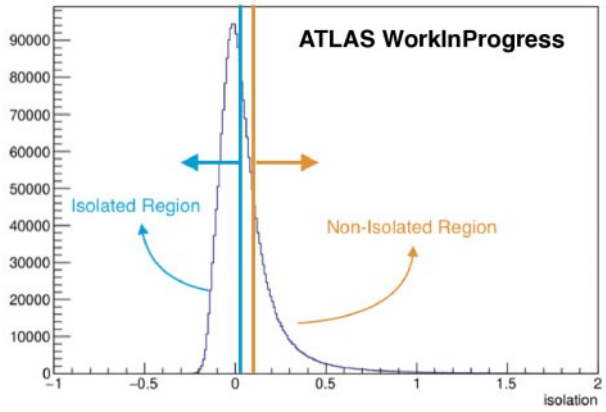

Fig. 4. – Extrapolated fake photons isolation distribution; the Isolated and Non-Isolated Regions used for fake factors calculation are highlighted.

TABLE I. – *Normalization factors for $Z(\to \nu\nu)\gamma$ and $W\gamma$ backgrounds extracted from the fit.*

m_T bin [GeV]	k_W	Error up	Error down
80-110	0.71	0.14	−0.11
110-140	0.69	0.12	−0.10
140-200	0.80	0.14	−0.11
200-300	1.11	0.17	−0.15

m_T bin [GeV]	k_Z	Error up	Error down
Inclusive	0.77	0.18	−0.16

TABLE II. – *Expected upper limit on $BR(H \to \gamma\gamma_d)$ at 95% CL.*

	-2σ	-1σ	Median	1σ	2σ
Expected limit	0.0103	0.0140	0.0196	0.0278	0.0384

$\to$T) that links tight and loose distributions (fig. 3) in MC is an affine transformation and it is related to the one that links tight and loose distributions in data ("L $\to$T").

Electrons faking photons backgrounds, with contributions from Z+jets and W+jets events, can enter the SR when prompt electrons are wrongly reconstructed and identified as photons, since their energy deposits in the electromagnetic calorimeter are very similar. This background category yield is estimated applying an electron-to-photon fake rate to events in a Probe-Electron CR, where 1 electron is required instead of 1 photon. The fake rate is computed using the $Z \to e^+e^-$ process, counting the events reconstructed as γe pairs with an invariant mass compatible with the Z boson mass.

5. – Statistical analysis

The statistical analysis is performed with a simultaneous fit in SR and CRs. In the following plots, the results of a blind fit in SR are shown. Data-driven estimations of jets faking photons and electrons faking photons backgrounds are included. The fit takes into consideration the systematic uncertainties on both data-driven fake photons estimations, and an arbitrary 10% flat systematic, applied to all other backgrounds so to mimic the foreseen effects of the experimental and theoretical uncertainties that will be included later.

Electrons faking photons are the dominant background in SR, followed by jets faking photons.

The expected upper limit on $BR(H \to \gamma\gamma_d)$ in this configuration is 1.96% (table II).

The plots in fig. 5 show the pre- and post-fit m_T distributions in SR, 1μCR and 2μCR. Using a binned k_W results in having a data/background ratio exactly equal to 1 in each bin, while an inclusive k_Z provides a less stable ratio, but still equal to 1 within 1σ. The values of the k-factors and their related statistical uncertainties are listed in table I.

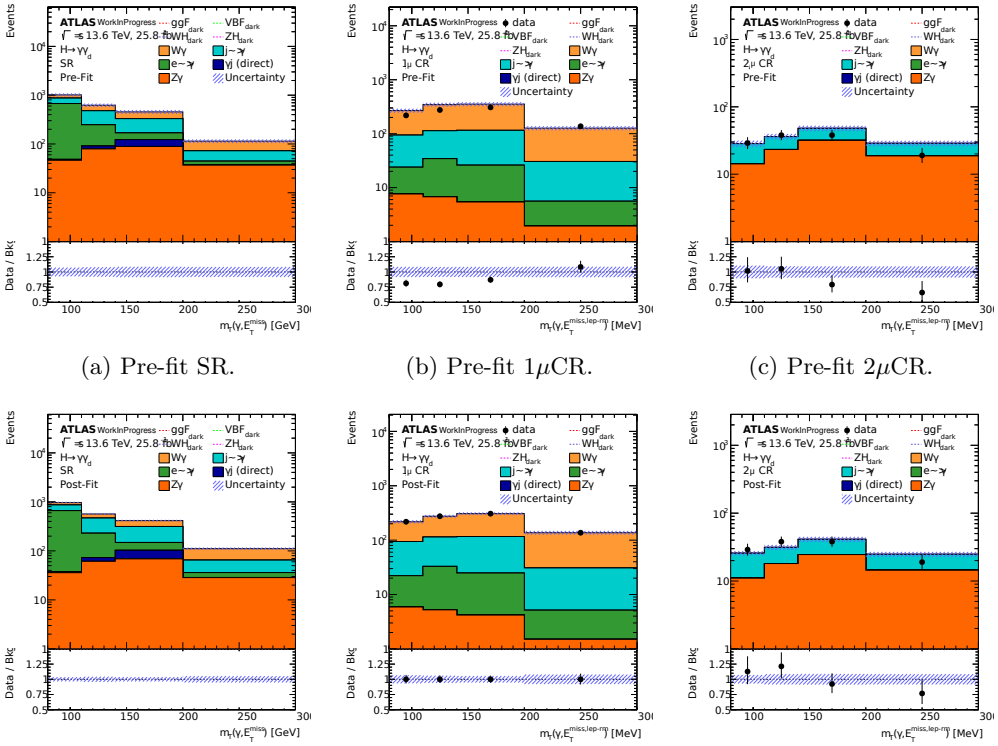

(a) Pre-fit SR. (b) Pre-fit 1μCR. (c) Pre-fit 2μCR.

(d) Post-fit SR. (e) Post-fit 1μCR. (f) Post-fit 2μCR.

Fig. 5. – Pre-fit and post-fit distributions in SR and CRs.

Nexts steps will be to include theoretical and experimental systematic uncertainties in the fit and combine the Run 3 result with the Run2 results obtained from VBF and ZH channels.

REFERENCES

[1] Freese K., *Int. J. Mod. Phys.*, **26** (2017) 1730012.

[2] Bertone G., Hooper D. and Silk J., *Phys. Rep.*, **405** (2005) 279.

[3] Ade P. A., Aghanim N., Alves M., Armitage-Caplan C., Arnaud M., Ashdown M., Atrio-Barandela F., Aumont J., Aussel H., Baccigalupi C. *et al.*, *Astron. Astrophys.*, **571** (2014) A1.

[4] Essig R., Jaros J. A., Wester W., Adrian P. H., Andreas S., Averett T., Baker O., Batell B., Battaglieri M., Beacham J., Beranek T., Bjorken J. D., Bossi F., Boyce J. R., Cates G. D., Celentano A., Chou A. S., Cowan R., Curciarello F., Davoudiasl H., deNiverville P., Vita R. D., Denig A., Dharmapalan R., Dongwi B., Döbrich B., Echenard B., Espriu D., Fegan S., Fisher P., Franklin G. B., Gasparian A., Gershtein Y., Graham M., Graham P. W., Haas A., Hatzikoutelis A., Holtrop M., Irastorza I., Izaguirre E., Jaeckel J., Kahn Y., Kalantarians N., Kohl M., Krnjaic G., Kubarovsky V., Lee H.-S., Lindner A., Lobanov A., Marciano W. J., Marsh D. J. E., Maruyama T., McKeen D., Merkel H., Moffeit

K., Monaghan P., Mueller G., Nelson T. K., Neil G. R., Oriunno M., Pavlovic Z., Phillips S. K., Pivovaroff M. J., Poltis R., Pospelov M., Rajendran S., Redondo J., Ringwald A., Ritz A., Ruz J., Saenboonruang K., Schuster P., Shinn M., Slatyer T. R., Steffen J. H., Stepanyan S., Tanner D. B., Thaler J., Tobar M. E., Toro N., Upadye A., de Water R. V., Vlahovic B., Vogel J. K., Walker D., Weltman A., Wojtsekhowski B., Zhang S. and Zioutas K., *Dark sectors and new, light, weakly-coupled particles* (2013).

[5] Gabrielli E., Heikinheimo M., Mele B. and Raidal M., *Phys. Rev. D*, **90** (2014) 055032.

[6] Fabbrichesi M., Gabrielli E. and Lanfranchi G., *The Physics of the Dark Photon: A Primer* (Springer International Publishing) 2021, https://link.springer.com/book/10.1007/978-3-030-62519-1.

[7] Aad G. *et al.*, *JINST*, **3** (2008) S08003.

[8] ATLAS Collaboration (Aad G. *et al.*), *Eur. Phys. J. C*, **80** (2020) 47.

[9] ATLAS Collaboration (Aad G. *et al.*), *J. Instrum.*, **15** (2020) P09015.

[10] ATLAS Collaboration (Aad G. *et al.*), *J. High Energy Phys.*, **2023** (2023) 133.

[11] ATLAS Collaboration (Aad G. *et al.*), *J. High Energy Phys.*, **2020** (2020) 80.

[12] ATLAS Collaboration (Aad G. *et al.*), *J. High Energy Phys.*, **2024** (2024) 153.

[13] CERN, *Sm higgs production cross sections at 13 tev*, accessed: 2024-06-24, https://twiki.cern.ch/twiki/bin/view/LHCPhysics/CERNYellowReportPageAt13TeV#SM_Higgs_production_cross_sectio.